Anti-echinococcal effect of verapamil involving the regulation of the calcium/calmodulin-dependent protein kinase Ⅱ response *in vitro* and in a murine infection model

Hai-Jun Gao
School of Basic Medical Sciences, Lanzhou University
Xu-Dong Sun
School of Basic Medical Sciences, Lanzhou University
Yan-Ping Luo
School of Basic Medical Sciences, Lanzhou University
Hua-Sheng Pang
National Health Commission Key Laboratory of Echinococcosis Prevention and Control, Xizang Center for Disease Control and Prevention
Xing-Ming Ma
School of Basic Medical Sciences, Lanzhou University
Ting Zhang (✉ zhangting@nipd.chinacdc.cn)
National Institute of Parasitic Diseases, China CDC
Tao Jing (✉ landa021001@126.com)
School of Basic Medical Sciences, Lanzhou Univeristy
Wei Hu
National Institute of Parasitic Disease, Chinese Center for Disease Control and Prevetion
Yu-Juan Shen
National Institute of Parasitic Diseases, Chinese Center for Disease Control and Prevetion
Jian-Ping Cao
National Institute of Parasitic Diseases, Chinese Center for Disease Control and Prevetion, WHO Collaborating Center for Tropical Diseases, National Center for International Research on Tropical Diseases, Key Laboratory of Parasitie and Vector Biology of the Chinese Ministry of Health

---

Research

Keywords: Verapamil, Echinococcus, Calmodulin, Calcium-calmodulin-dependent protein kinases

Posted Date: January 29th, 2021

DOI: https://doi.org/10.21203/rs.3.rs-107151/v2

Version of Record: A version of this preprint was published at Parasites & Vectors on February 15th, 2021.
See the published version at https://doi.org/10.1186/s13071-021-04618-4.

Abstract

Background: Echinococcosis caused by the larvae of cestodes of the genus *Echinococcus* is a parasitic zoonosis that poses a serious threat to the health of humans and animals globally. Albendazole is the drug of choice for the treatment of echinococcosis, but it is difficult to meet clinical goals with this chemotherapy due to its low cure rate and the assocaiated side effects after long-time use. Hence, novel anti-parasitic targets and effective treatment alternatives are urgently needed. A previous study showed that verapamil can suppress the growth of *Echinococcus granulosus* larvae; however, the mechanism of this effect remains unclear. The aim of the present study was to gain insight into the anti-echinococcal effect of verapamil on *Echinococcus* with a particular focus on the regulatory effect of verapamil on calcium/calmodulin-dependent protein kinase Ⅱ (Ca^{2+}/CaM-CamKⅡ) in infected mice.

Methods: The anti-echinococcal effects of verapamil on *E. granulosus* protoscoleces (PSC) *in vitro* and *E. multilocularis* metacestodes in infected mice were assessed. The morphological alterations in *Echinococcus* spp. induced by verapamil were observed by scanning electron microscopy (SEM), and the changes in calcium content in both the parasite and mouse serum and liver were measured by SEM-energy dispersive spectrometry, inductively coupled plasma mass spectrometry and Alizarin red staining. Additionally, the changes in the protein and mRNA levels of CaM and CamKⅡ in infected mice, and in the mRNA levels of *CamKⅡ* in *E. granulosus* PSC were evaluated after treatment with verapamil by immunohistochemistry and/or real-time quantitative polymerase chain reaction.

Results: *In vitro*, *E. granulosus* PSC could be killed by verapamil at a concentration of 0.5 μg/mL or higher within 8 days. Under these conditions, the ultrastructure of PSC was damaged, and this damage was accompanied obvious calcium loss and downregulation of *CamKⅡ* mRNA expression. *In vivo*, the weight and the calcium content of *E. multilocularis* metacestodes from mice were reduced after treatment with 40 mg/kg verapamil, and an elevation of the calcium content in the sera and livers of infected mice was observed. In addition, downregulation of CaM and CamKⅡ protein and mRNA expression in the livers of mice infected with *E. multilocularis* metacestodes was found after treatment with verapamil.

Conclusions: Verapamil exerted a parasiticidal effect against *Echinococcus* both *in vitro* and *in vivo* through downregulating the expression of Ca^{2+}/CaM-CamKⅡ, which were over-activated by parasitic infection. The results suggested that Ca^{2+}/CaM-CamKⅡ may be a novel drug-target, and verapamil was shown to be a potential anti-echinococcal drug for controlling echinococcosis in the future.

Background

Echinococcosis is a serious but neglected helminthic zoonosis caused by the genus *Echinococcus*, mainly *Echinococcus granulosus*, which causes cystic echinococcosis (CE), and *E. multilocularis*, which causes alveolar echinococcosis (AE) [1]. CE occurs globally, and AE occurs in the Northern Hemisphere and imposes a heavy disease burden [2]. According to previous data from central Asia, at least 270 million people are exposed to *Echinococcus*, and the prevalence of the disease in some Tibetan areas of

western China ranges from 0.8% to 11.9% [3]. Notably, higher pathogenicity and case fatality rate are associated with AE due to its tumour-like growth [3]. The clinical treatment strategies for echinococcosis include surgical operation and drug chemotherapy. Albendazole (ABZ) is a benzimidazole derivatives and the prime chemotherapeutic drug used for the treatment of human echinococcosis [4], and it exerts an anti-parasitic effect by disrupting microtubule polymerization and biochemical processes, such as glucose and energy metabolism, in the parasite [5]. However, ABZ exerts parasitostatic rather than parasiticidical effects [6], has poor gastrointestinal absorption and it associated with severe side effects [7, 8]. Hence, new drugs for the treatment of this parasitosis have been investigated, such as traditional Chinese medicines from some botanical extracts [9], antineoplastic chemotherapeutics [7, 10], and immunosuppressants [11, 12]. However, only a few of these agents, such as mefloquine and amphotericin B alone or in combination with nitazoxanide, have been used as auxiliary treatments for human echinococcosis [6]. Therefore, investigation of novel anti-*Echinococcus* drugs and drug targets is urgently needed.

Ca^{2+}, a pivotal second messenger, controls the physiological process in cells, such as proliferation, differentiation and migration [13]. The complex consisting of Ca^{2+} and calmodulin (CaM) can specifically bind to CaM-dependent protein kinases (CamKs, including CamK□, CamK□, CamK□ and CamK□) to activate the Ca^{2+}/CaM-CamKs cascade, which can promote signal transduction in cells [14]. Previous studies in tumours have shown that the Ca^{2+}/CaM-CamK cascade controls tumorigenesis and tumour progression [13, 15, 16]. Furthermore, the Ca^{2+}/CaM-CamKs cascade has been suggested to be closely related to the pathogenesis of many hepatic parasites. For example, in *Schistosoma mansoni*, the IQ motif of SmCav1B, which is a voltage-gated calcium channel, can interact with two CaMs, SmCaM1 and SmCaM2, to promote growth [17], and RNAi silencing of a calcium-regulated protein affects the morphology and vitality of *S. japonicum* [18]. Two voltage-gated calcium channel β-subunits, $CsCa_v\beta1$ and $CsCa_v\beta2$, boost the parasiticidal effect of praziquantel on *Clonorchis sinensis* [19], and *Fh*CaM dyshomeostasis can obviously block the growth and motility in *Fascida hepatica* [20]. Therefore, Ca^{2+}/CaM-CamKs have become potential therapeutic targets in cancers and parasitosis, and calcium channel inhibitors, such as verapamil and praziquantel, have been confirmed to have anti-tumorigenic and anti-parasitic effects [13, 15, 21, 22]. Furthermore, verapamil has been shown to alleviate atrial fibrillation in rats by downregulating the expression of overactivated Cav1.2-CaM-CaMK□ [23]. In *E. granulosus* PSC, the presence of calcareous corpuscles indicate that calcium sources are required for hydatid cyst development [24], and the calcium level in hydatid cysts has been shown to be higher than that in the serum or plasma of the host [25]. Previous studies has preliminarily confirmed that verapamil suppresses the growth of *E. granulosus* larvae [26, 27]; however, it is unclear whether the compound has similar anti-parasitic effects on *E. multilocularis*, which is a tumour-like parasite more harmful to humans. The mechanism of action of verapamil against *Echinococcus* has never been investigated, and it is unclear whether the inhibitory effects of verapamil on *E. granulosus* are mediated by the regulation of Ca^{2+}/CaM-CamK□. Hence, this study aimed to investigate the efficacy and mechanism of action of verapamil against *Echinococcus*.

Methods

Biochemical reagents

Verapamil (V111249), ABZ (A131023), albendazole sulfoxide (ABZ-SO, 35395) and pentobarbital sodium were purchased from Sigma (Missouri, US) and Aladdin (Shanghai, China). Antibodies and PCR primers were purchased from Abcam (Cambridge, US) and Beijing Genomics Institute (Beijing, China). Enzyme-linked immunosorbent assay (ELISA) kits for CaM and CaMK were purchased from CUSABIO (Wuhan, China). All culture reagents were purchased from Gibco (Wisent, Canada). Extraction kits for total RNA and PCR kits were purchased from Takara (Tokyo, Japan).

Separation and culture of *E. granulosus* PSC *in vitro*

E. granulosus PSC were obtained from the livers of naturally infected sheep from the slaughterhouse of Xining City, Qinghai Province, China, rinsed with phosphate buffered saline (PBS), resuspended in Dulbecco's modified Eagle's medium (DMEM) containing 1% penicillin-streptomycin (P-S), and then incubated in 24-well culture plates (100 PSC per well) at 37 ℃, 5% CO_2. Morphological alterations in PSC were observed under an inverted microscopy (BX43, Olympus, Japan), and the survival rate of PSC was recorded daily.

Mouse infection with *E. multilocularis*

Kunming mice 6-8 weeks of age were purchased from the Laboratory Animal Center of Lanzhou University and housed in a HEPA-filtered and temperature-controlled environment on a light/dark cycle at 22-25 ℃. The mice were fed a rodent diet (Beijing Keao, Beijing, China) *ad libitum* under specific pathogen-free (SPF) laboratory conditions. *E. multilocularis* PSC were aseptically isolated from anaesthetized *E. multilocularis*-infected gerbils in our laboratory as described previously [28] to establish a murine infection model by in situ surgical intrahepatic implantation. Healthy mice (n = 15) were infected with *E. multilocularis* PSC (1,500 PSC per mouse) in the SPF laboratory, and other mice (n = 5), which were used as the uninfected group, were subjected to a sham procedure; both groups were housed under the same conditions.

Drug treatment *in vitro*

The experimental animals were divided into (i) the vehicle group, which was treated with 0.1% dimethylsulfoxide (DMSO) (n = 3); (ii) the ABZ-SO group, which was treated with 40 and 20 μg/mL ABZ-SO dissolved in 0.1% DMSO (n = 3); and (iii) the verapamil groups, which were treated with 100, 80, 40, 20, 10, 5, 2, 1 or 0.5 μg/mL verapamil (n = 3). After drug treatment, *E. granulosus* PSC were stained with 0.4% trypan blue for 10 min to observe morphological changes. In addition, *E. granulosus* PSC were fixed with 4% glutaraldehyde, rinsed with PBS (1×), and stained with 2% osmium tetroxide for 2 hours and 1% uranyl acetate for 30 min. Subsequently, these specimens were dehydrated in increasing concentrations

of ethanol, air-dried and coated with gold as described previously [28]. Finally, the microstructure of the PSC was observed under a scanning electron microscopy (SEM, JSM-5600LV, JEOL, Japan).

Drug treatment *in vivo*

Three months after infection with *E. multilocularis* PSC, all infected mice were divided into the following groups for oral drug administration: (i) the group of infected mice treated daily with honey/PBS (1:1 v/v) (n = 5); (ii) the group of ABZ mice treated daily with 40 mg/kg ABZ in honey/PBS (1:1 v/v) (n = 5); (iii) the group of mice were treated daily with 40 mg/kg verapamil in honey/PBS (1:1 v/v) (n = 5); and (iv) the group of uninfected mice treated daily with honey/PBS (1:1 v/v) (n = 5). After four months of treatment, *E. multilocularis* cysts, sera and livers were harvested from the mice to measure the calcium content and CaM and CamK protein and mRNA expression.

Calcium content analysis by ICP-MS, SEM-EDS and Alizarin red staining

(i) For inductively coupled plasma mass spectrometry (ICP-MS) analysis, equal amounts of tissue or serum/culture supernatant samples were prepared for calcium analysis. Tissue digestion was performed with a microwave digestion system using UltraClave (Milestone, Sorisole, Italy), and sample analysis was performed as described previously [29].

(ii) For scanning electron microscopy-energy dispersive X-ray spectroscopy (SEM-EDS) analysis, changes in the calcium content in *E. granulosus* PSC and in the germinal layer cells of *E. multilocularis* metacestodes were observed after treatment with verapamil by a LEO Gemini field emission gun scanning electron microscopy (FEG-SEM, JEOL, Japan) as described previously [30].

(iii) For Alizarin red staining, *E. multilocularis* metacestodes and mouse livers were fixed with 4% paraformaldehyde for 2 weeks, and then stained with Alizarin red to detect calcification as described previously [31]. The percentage of positively stained calcium deposits in the images was calculated by using ImageJ software (National Institutes of Health, Bethesda, MD, USA).

Analysis of CaM and CamK protein expression analysis by IHC-P and ELISA

(i) For paraffin-immunohistochemistry (IHC-P), 4 μm thick sections of *E. multilocularis* metacestodes and mouse livers were processed to evaluate the expression of CaM or CamK as described previously [32, 33]; immunostaining was performed using rabbit anti-CaM/CamK antibodies (Bioss, Beijing, China) at a 1:300/1:200 dilution and secondary antibodies (goat anti-rabbit IgG, Bioss, Beijing, China) at a 1:800 dilution. Finally, the slides were imaged under a fluorescence microscopy (Olympus, Japan). Semiquantitative analysis was performed by using ImageJ software.

(ii) For ELISA, PBS (pH = 7.2) containing PMSF (10 mmol/L) was added to serum and tissue samples, which were then rapidly homogenised and centrifuged at 1,000 ´ *g* for 10 min to measure the protein concentrations of CaM and CamK according to the ELISA kit protocols.

Analysis of *CaM* and *CamKⅡ* mRNA expressionby RT-qPCR

The expression of *CaM* or/and *CamKⅡ* mRNA in *E. granulosus* PSC, mouse livers and *E. multilocularis* cysts was measured by real-time quantitative polymerase chain reaction (RT-qPCR), and *β-actin* mRNA was used as an internal standard. Nucleic acid was isolated from various tissues by using TRIzol reagent (Invitrogen, San Diego, USA), and reverse-transcribed into cDNA; amplification of cDNA was performed by RT-qPCR as described by the Takara kit protocols (no. RR036A). The following primers were used: *Eg-CamKⅡ/Em-CamkⅡ* (forward, 5'-TCGTTGTTCAAGTCGGTTCG-3'; reverse, 5'-GGTGCTGAGAGACCCACTAG-3'), *Eg-β-actin/Em-β-actin* (forward, 5'-AGACATCAGGGAGTGATGGTT-3'; reverse, 5'-GAGGACTGGATGCTCCTCAGG-3'); *mouseCamKⅡ* (forward, 5'-GGCCTGGACTTT-CATCGATTCTA-3'; reverse, 5'-CATCAGGTGGATGTGAGGGTTC-3'), mouse *CaM* (forward, 5'-AAGCCGAGCTGCAGGATATGA-3'; reverse, 5'-CAGTTCTGCCGCACTGATGTAA-3'), and mouse *β-actin* (forward, 5'-TTGTTACCAACTGGGACG-3'; reverse, 5'-GGCATAGAGGTCTTTACGG-3').

Statistical analysis

The data are presented as the mean ± standard deviation (SD). Statistical differences between the groups were assessed by t-test and paired comparisons. Statistical analysis was performed by SPSS version 22.0 (IBM Corp., Chicago, USA) and GraphPad Prism version 7.0 (GraphPad Software, Inc., San Diego, CA, USA). $P < 0.05$ indicated significant differences.

Results

Effect of verapamil on *E. granulosus* PSC *in vitro*

The survival rate of *E.granulosus* PSC after treatment with various concentrations of verapamil (0.5, 1, 2, 5, 10, 20, 40, 80 or 100 μg/mL) within 8 days is shown in Fig. 1A. The mortality of PSC upon exposure to 0.5-40 μg/mL verapamil was time-dependent; all PSC were killed within 2 days by 40 μg/mL verapamil or within 4 days by 20 μg/mL verapamil. However, ABZ-SO had killed only 13% of PSC on day 2 when administrated at a concentration of 40 μg/mL and 21% of PSC on day 4 when administrated at a concentration of 20 μg/mL; 4% of PSC in the vehicle group were dead on day 2, and 8% of PSC were dead on day 4.

Comparison of the natural morphology of PSC with those in the vehicle group by light microscopy showed mild alterations in PSC in the ABZ-SO (20 μg/mL) group and substantial morphological alterations (i.e., disappearance of calcareous corpuscles) of PSC after exposure to 20 μg/mL verapamil for 4 days (Fig. 1Ba-c). Additionally, PSC in the verapamil (20 μg/mL) group were stained with trypan blue on day 4, unlike the viable PSC in the ABZ-SO (20 μg/mL) and vehicle group (Fig. 1Bd-f). According to SEM, the ultrastructural changes that occurred in PSC exposed to verapamil (20 μg/mL) for 4 days were shedding of the tegument, disappearance of hooks and the presence of numerous blebs; however, PSC in the vehicle and ABZ-SO (20 μg/mL) groups remained intact (Fig. 1Bg-i).

Changes in the calcium content in *E. granulosus* PSC exposed to verapamil *in vitro*

The calcium distribution in *E. granulosus* PSC treated with verapamil (20 μg/mL) for 4 days were heterogeneous and sparse compared with those in the vehicle group, as determined by SEM-EDS (Fig. 2A). Semiquantitative analysis showed that the calcium level in PSC decreased after treatment with verapamil (Fig. 2B). In addition, an obvious dose-dependent increase in the calcium content in the culture supernatant of the verapamil group compared with the vehicle group was observed (Fig. 2C).

Effect of verapamil on *E. multilocularis* metacestodes *in vivo*

E. multilocularis-infected mice were treated with verapamil (40 mg/kg) or ABZ (40 mg/kg) for 4 months *in vivo*. The wet weights of *E. multilocularis* cysts isolated from the verapamil (0.98 ± 0.33 g) and ABZ groups (1.04 ± 0.14 g) were significantly decreased compared with those of cysts from the infected group (5.90 ± 0.75 g) ($P = 0.000$, Table 1).

Changes in the calcium concentration in *E. multilocularis* infected mice after verapamil treatment

The calcium concentration in the sera of *E. multilocularis*-infected mice was 4.92 ± 0.77 mg/L, which represented a 2-fold decrease compared with that in the uninfected group (9.89 ± 1.92 mg/L); treatment with verapamil for 4 months induced a recovery of the calcium concentration to 6.39 ± 0.79 mg/L (Table 2). Similarly, the level of calcium in the livers of mice decreased from 296.72 ± 9.43 mg/L to 172.72 ± 16.63 mg/L due to *E. multilocularis* metacestode infection. Interestingly, the calcium content in the liver increased to 226.78 ± 43.93 mg/L after treatment with verapamil ($P = 0.009$). Additionally, the results of the ICP-MS assay showed that the calcium level in *E. multilocularis* cysts isolated from the infected group was 3182.28 ± 190.77 mg/L; this level decreased to 3013.98 ± 115.80 mg/L after treatment with verapamil for 4 months ($P = 0.13$). Additionally, changes in the calcium level in *E. multilocularis* cysts were evaluated by SEM-EDS (Fig. 3A), and the percentage of calcium weight in *E. multilocularis* cysts rapidly decreased from 14.28% to 8.66% after treatment with verapamil; these differences were statistically significant ($P = 0.000$) (Fig. 3B). The results of Alizarin red staining showed that calcium deposition around the portal area of the liver in infected mice was significantly increased compared with that in the uninfected group (Fig. 4). The decrease in calcium content in the infected liver was not reversed by treatment with verapamil. The calcium content in *E. multilocularis* cysts was not obviously reduced ($P > 0.05$), however, a reduction in the number of PSC was observed.

Analysis of CaM and CamKⅡ protein levels in *E. multilocularis*-infected mice treated with verapamil

IHC-P staining revealed high expression of CaM in the livers of infected mice compared with those of uninfected mice (Fig. 5A); however, pathological progression was inhibited by verapamil, and the differences were statistically significant ($P < 0.05$). Furthermore, ELISA showed that the CaM protein concentration in the mouse serum and liver increased significantly from 13.81 ± 1.65 to 22.25 ± 5.55 μg/mL and from 3.42 ± 0.27 to 6.06 ± 1.83 μg/mL, respectively, after *E. multilocularis* infection; however, after treatment with verapamil, CaM protein expression was obviously inhibited in the serum (8.13 ± 1.26

μg/mL) and liver (1.60 ± 0.68 μg/mL) but not in the cysts (from 2.36 ± 0.87 to 1.68 ± 0.10 μg/mL) (Table 3).

Similar to that of CaM, the IHC-P assay indicated that the overexpression of CamKⅡ in the livers and cysts in *E. multilocularis*-infected mice was significantly suppressed by verapamil treatment (Fig. 5B). Additionally, an increase in CamKⅡ content in the mouse serum (22.87 ± 4.23 ng/mL) and liver (4.25 ± 1.84 ng/mL) was observed after *E. multilocularis* infection, and these values were decreased to 5.13 ± 1.74 ng/mL and 1.97 ± 0.56 ng/mL, respectively, after verapamil treatment. However, only a mild decrease in CamKⅡ content in the cysts (from 2.65 ± 1.24 to 1.79 ± 0.36 ng/mL) was observed after verapamil treatment ($P > 0.05$, Table 3).

Analysis of *CaM* and *CamKⅡ* mRNA expression in the parasite and in *E. multilocularis*-infected mice after treatment with verapamil

The changes in Ca^{2+}/CaM-CamKⅡ expression in parasite-infected mice after treatment with verapamil were evaluated based on the changes in *CaM* and/or *CamKⅡ* mRNA expression in the mouse liver and in *Echinococcus*, as measured by using RT-qPCR. The data shown in Fig. 6A-B indicate that *CaM* and *CamKⅡ* mRNA expression in the mouse liver was increased by 4-fold and 6-fold, respectively, after infection with *Echinococcus*. Overexpression of *CaM* and *CamKⅡ* mRNA in the liver was significantly suppressed by verapamil ($P = 0.000$). After treatment with verapamil, *CamKⅡ* mRNA expression was obviously downregulated, while *CaM* mRNA expression was mildly reduced ($P > 0.05$). Furthermore, *CamKⅡ* mRNA expression in *E. granulosus* PSC exposed to verapamil *in vitro* was obviously downregulated (Fig. 6C).

Discussion

E. granulosus andE. multilocularis metacestodes are inclined to parasitize the liver; and *E. multilocularis* metacestodes, which exhibit tumour-like growth, become more noticeable and lead to death if untreated [34]. While its intestinal absorption is poor and it is associated with severe side effects [7], ABZ, which exerts a parasitostatic rather than a parasitocidical effect, has long been used to treat human echinococcosis. Hence, mew anti-echinococcal targets and therapeutic options should be urgently explored.

The Ca^{2+}/CaM-CamKs pathway is a potential therapeutic target for cancers and is closely monitored in many cases of parasitosis; however, it is unclear how Ca^{2+}/CaM-CamKⅡ regulates the growth and development of *Echinococcus* spp. and needs to be explored to identify potential drugs for the treatment of echinococcosis at early stages.

The results of the present study indicated that the anti-echinococcal effect of verapamil on *E. granulosus* PSC was time- and dose-dependent, similar to the inhibitory effects of this drug on tumour proliferation. Calcareous corpuscles in PSC can persistently provide abundant calcium sources to promote PSC development into cysts [24]. In the present study, rapid disappearance of calcareous corpuscles and a

decrease in the calcium content in *E. granulosus* PSC were induced by exposure to verapamil, indicating that verapamil kills *E. granulosus* PSC by promoting calcium loss.

AE is usually called “parasitic cancer” due to distinctive its tumour-like growth, and approximately 70% of the metacestodes are found in the right lobe of the patient’s liver. The germinal layer cells in *E. multilocularis* metacestodes have high regenerative capacity and can develop into new multicellular structures, such as PSC, which can further develop into new metacestodes. Therefore, *E. multilocularis* metacestodes can infiltrate the whole liver of the host [35]. In this study, an infection model was established by *in situ* surgical intrahepatic implantation to recapitulate the natural onset and development of AE in mice as closely as possible. After *E. multilocularis*-infected mice were treated with 40 mg/kg verapamil for 4 months, the weight of *E. multilocularis* cysts was significantly decreased, suggesting that the growth of metacestodes was suppressed. This finding is similar to the results of the study by Cao on the effect of verapamil in mice with CE [26]. Infection with *E. multilocularis* metacestodes was reported to reduce serum calcium levels in both mice and humans [25, 36]. Interestingly, our results revealed that the reduction in the calcium content in *E. multilocularis*-infected mice was significantly reversed after administration of verapamil, and an apparent mild increase was observed in the liver but not in the serum or cysts. The calcium content in *E. multilocularis* metacestodes was substantially higher than that in the host liver and serum, indicating that the development of *E. multilocularis* PSC into metacestodes requires continuous absorption of calcium from the host. Furthermore, the results of the SEM-EDS assay showed that treatment with verapamil obviously reduced the calcium content and the number of germinal layer cells. Thus, we speculated that the proliferation of germinal layer cells is regulated by the calcium supply in infected mice and can be disrupted by the calcium channel inhibitor verapamil. However, the detailed mechanism by which verapamil suppresses the growth of germinal layer cells by regulating the Ca^{2+}/CaM-CamKs cascade requires additional investigation. Furthermore, the results of Alizarin red staining and ICP-MS suggested that *E. multilocularis* metacestodes cause calcium translocation from mice into the parasite, and a calcium channel inhibitor (verapamil) rescued calcium loss in *E. multilocularis*-infected mice. In addition, abundant lymphocytes surrounded the *E. multilocularis* cysts in the liver after treatment with verapamil, which may be associated with an increase in the calcium content in the livers of *E. multilocularis*-infected mice after treatment with verapamil, probably because a sufficient level of calcium can promote the proliferation and polarization of T cells [37]; however, the abnormal changes in lymphocyte development caused by calcium loss in *Echinococcus*-infected hosts requires further investigation.

Our results indicated that an increase in the expression of CaM and CamK□ proteins in mouse serum and liver was caused by *E. multilocularis* metacestode infection; however, overexpression of the CaM and CamK□ proteins was significantly suppressed by verapamil. Furthermore, the expression of *CaM* and *CamK□* mRNA in the mouse liver and *E. multilocularis* metacestodes was downregulated after treatment with verapamil. Our results partially support the recent findings of Sujeevi S. K. Nawaratna, who showed that Ca^{2+}/CaM-CamK□ is a putative therapeutic target for helminth parasite infection that can provide biochemical and pharmacological information for exploring novel compounds in the future [38].

Ca^{2+}/CaM-CamK□ controls the completion of the life cycle in *Echinococcus*, and the calcium channel blocker verapamil has strong inhibitory effects against *Echinococcus*, including germinal layer cells, PSC and metacestodes. Therefore, subsequent studies should evaluate the molecular and immune mechanisms of the effects of verapamil on the over-activation of the Ca^{2+}/CaM-CamK□ pathway in *Echinococcus*-infected hosts. Furthermore, novel anti-echinococcal drug targets and effective treatment strategies associated with Ca^{2+}/CaM-CamK□ should be carefully investigated.

Conclusions

The results of our study suggest that verapamil has parasiticidal effects on *E. granulosus* PSC *in vitro* by promoting calcium loss and on *E. multilocularis* metacestodes *in vivo* by inhibiting calcium translocation from mice to parasites. Furthermore, Ca^{2+}/CaM-CamK□ in the mouse is overactivated by *Echinococcus* infection, and this effect is alleviated by oral administration of verapamil. Thus, our findings provide new information by identifying Ca^{2+}/CaM-CamK□ as the targets of the anti-*Echinococcus* effects of verapamil. Subsequent investigation of the functions of Ca^{2+}/CaM-CamK□ in the growth and development of *Echinococcus* and the chronic toxicity of verapamil are currently in progress in our laboratory.

Abbreviations

Vepm, verapamil; AE, alveolar echinococcosis; PSC, protoscoleces; ABZ, aldendazole; DMSO, dimethylsulfoxide; CaM, calmodulin; CamK□, Ca^{2+}/calmodulin dependent protein kinase □; ABZ-SO, albendazole sulfoxide; IHC-P, immunohistochemistry-paraffin; PBS, phosphate buffered saline; SEM-EDS, scanning electron microscopy and energy dispersive spectrometer; ICP-MS, inductively coupled plasma mass spectrometry; RT-qPCR, real-time quantitative polymerase chain reaction; ELISA, enzyme-linked immuno-sorbent assay.

Declarations

Ethics approval and consent to participate

This study was conducted in accordance with the Chinese Laboratory Animal Administration Act and the study protocol was approved by the Experimental Animal Ethics Committee of School of Basic Medical Sciences, Lanzhou University (permit no. 2014-12-003).

Consent for publication

Not applicable.

Availability of data and materials

The Datasets supporting the conclusions of this article are included within the article.

Competing interests

The authors declare that they have no competing interests.

Funding

This study was financially supported by the Foundation of National Science and Technology Major Program (No. 2018ZX10713001-004), National Natural Science Foundation of China (No. 81171632 and 81201315), the Fundamental Research Funds for the Central Universities (No. lzujbky-2014-m02) and the Foundation of Shanghai Municipal Health Commission (No. 201940302) and the Non-profit Central Research Institute Fund of Chinese Academy of Medical Sciences (No. 2019PT320004). The funders had no role in the study design, data collection, data analysis, data interpretation, or the writing of this report.

Authors' contributions

TJ, TZ and HJG conceived and designed the experiments; HJG and YPL performed the experiments; HJG, TZ, WH, XMM, YJS, JPC analyzed the data and contributed reagents and materials, XDS and HSP participated in animal model; HJG, TZ wrote the paper. All authors have read and approved the final version of the manuscript.

Acknowledgments

The authors would like to thank Dr. HB Zhang, B Jiang and LL Huo (National Institute of Parasitic Diseases, Chinese Center for Disease Control and Prevention, Key Laboratory of Parasite and Vector Biology, MOH, National Center for International Research on Tropical Diseases, WHO Collaborating Centre for Tropical Diseases, China) for the technical assistance.

Author details

[1]School of Basic Medical Sciences, Lanzhou University, Lanzhou 730000, Gansu Province, People's Republic of China.

[2]National Institute of Parasitic Diseases, Chinese Center for Disease Control and Prevention, WHO Collaborating Center for Tropical Diseases, National Center for International Research on Tropical Diseases, Key Laboratory of Parasite and Vector Biology of the Chinese Ministry of Health, Shanghai 200025, People's Republic of China.

[3]Ganzr Tibetan Autonomous Prefecture Center for Disease Control and Prevention, Kangding 626000, Sichuan Province, People's Republic of China.

[4]National Health Commission Key Laboratory of Echinococcosis Prevention and Control, Xizang Center for Disease Control and Prevention, 21 Linkuo North Road, Lhasa 850000, Tibet Autonomous Region, People's Republic of China.

References

1. Wang H, Li J, Guo B, Zhao L, Zhang Z, McManus DP, et al. In vitro culture of *Echinococcus multilocularis* producing protoscoleces and mouse infection with the cultured vesicles. Parasit Vectors. 2016;9:411.
2. Romig T, Deplazes P, Jenkins D, Giraudoux P, Massolo A, Craig PS, et al. Ecology and Life Cycle Patterns of Echinococcus Species. Adv Parasitol. 2017;95:213-314.
3. Li ZD, Mo XJ, Yan S, Wang D, Xu B, Guo J, et al. Multiplex cytokine and antibody profile in cystic echinococcosis patients during a three-year follow-up in reference to the cyst stages. Parasit Vectors. 2020;13:133.
4. Kern P, Menezes da Silva A, Akhan O, Mullhaupt B, Vizcaychipi KA, Budke C, et al. The Echinococcoses: Diagnosis, Clinical Management and Burden of Disease. Adv Parasitol. 2017;96:259-369.
5. Horton J. Albendazole: a review of anthelmintic efficacy and safety in humans. Parasitology. 2000;121: S113-32.
6. Fabbri J, Pensel PE, Albani CM, Arce VB, Martire DO, Elissondo MC. Drug repurposing for the treatment of alveolar echinococcosis: in vitro and in vivo effects of silica nanoparticles modified with dichlorophen. Parasitology. 2019; 146:1620-30.
7. Yuan M, Luo Y, Xin Q, Gao H, Zhang G, Jing T. Efficacy of osthole for *Echinococcus granulosus* in vitro and *Echinococcus multilocularis* in vivo. Vet Parasitol. 2016;226:38-43.
8. Stamatakos M, Sargedi C, Stefanaki C, Safioleas C, Matthaiopoulou I, Safioleas M. Anthelminthic treatment: an adjuvant therapeutic strategy against *Echinococcus granulosus*. Parasitol Int. 2009;58:115-20.
9. Abdel-Baki AA, Almalki E, Mansour L, Al-Quarishy S. In Vitro Scolicidal Effects of Salvadora persica Root Extract against Protoscolices of *Echinococcus granulosu* Korean J Parasitol. 2016;54:61-6.
10. Nicolao MC, Elissondo MC, Denegri GM, Goya AB, Cumino AC. *In vitr*o and in vivo effects of tamoxifen against larval stage *Echinococcus granulosus*. Antimicrob Agents Chemother. 2014;58:5146-54.
11. Colebrook AL, Jenkins DJ, Jones MK, Tatarczuch L, Lightowlers MW. Effect of cyclosporin A on the survival and ultrastructure of *Echinococcus granulosus* protoscoleces *in vitro*. Parasitology. 2004;129:497-504.
12. Reuter S, Merkle M, Brehm K, Kern P, Manfras B. Effect of amphotericin B on larval growth of *Echinococcus multilocularis*. Antimicrob Agents Chemother. 2003;47:620-5.
13. Iamshanova O, Fiorio Pla A, Prevarskaya N. Molecular mechanisms of tumour invasion: regulation by calcium signals. J Physiol. 2017;595:3063-75.
14. Billker O, Lourido S, Sibley LD. Calcium-dependent signaling and kinases in apicomplexan parasites. Cell Host Microbe. 2009;56:612-22.

15. Cui C, Merritt R, Fu L, Pan Z. Targeting calcium signaling in cancer therapy. Acta Pharm Sin B. 2017;71:3-17.
16. Hu Y, Liu P, Kang L, Li J, Li R, Liu T. Mechanism of Marsdenia tenacissima extract promoting apoptosis of lung cancer by regulating Ca(2+)/CaM/CaMK signaling. J Ethnopharmacol. 2020;251:1125-35.
17. Thomas CM, Timson DJ. Calmodulins from *Schistosoma mansoni*: Biochemical analysis and interaction with IQ-motifs from voltage-gated calcium channels. Cell Calcium. 2018;74:1-13.
18. Zou X, Jin Y-m, Liu P-p, Wu Q-j, Liu J-m, Lin J-j. RNAi silencing of calcium-regulated heat-stable protein of 24 kDa in *Schistosoma japonicum* affects parasite growth. Parasitology Research. 2010;108 3:567-72.
19. Cho PY, Yoo WG, Kim TI, Ahn SK, Cho SH, Kim TS, et al. Molecular characterization of voltage-gated calcium channel beta-subunits of *Clonorchis sinensis*. Parasitol Res. 2014;113 1:121-9.
20. McCammick EM, McVeigh P, McCusker P, Timson DJ, Morphew RM, Brophy PM, et al. Calmodulin disruption impacts growth and motility in juvenile liver fluke. Parasit Vectors. 2016;9:46.
21. Zhao L, Zhao Y, Schwarz B, Mysliwietz J, Hartig R, Camaj P, et al. Verapamil inhibits tumor progression of chemotherapy-resistant pancreatic cancer side population cells. Int J Oncol. 2016;49 1:99-110.
22. Harun MSR, Marsh V, Elsaied NA, Webb KF, Elsheikha HM. Effects of *Toxoplasma gondii* infection on the function and integrity of human cerebrovascular endothelial cells and the influence of verapamil treatment in vitro. Brain Res. 2020;1746: 147002.
23. Zhang YT, Hu HH, Chen W, Shi S, Weng W. Influence of wenxin granule on atrial myocytes calcium-handling CaV1.2-CaM-CaMK signal pathway of atrial brillation rat. China journal of traditional Chinese medicine and pharmacy. 2017;32(5):2246-9. (in Chinese)
24. Rodrigues JJS, Ferreira HB, Farias SE, Zaha A. A protein with a novel calcium-binding domain associated with calcareous corpuscles in *Echinococcus granulosus*. Biochemical & Biophysical Research Communications. 1997; 237(2):451-6.
25. Desser SS. Calcium accumulation in larval *Echinococcus multilocularis*. Canadian Journal of Zoology. 1963; 41(6):1055-9.
26. Cao D, Bai H, Zhao H. Effects of verapamil hydrochloride on the ultrastructures of secondary cysts of *Echinococcus granulosus* in mice. Journal of parasitic biology. 2010;5(6): 448-9. (in Chinese)
27. Cao D, Shi D, Bao G. Observation on verapamil and albendazole against *Echinococcus granulosus* protoscolex *in vitro*. Endemic Disease Bulletin (China). 2004; 19(1):23-24. (in Chinese)
28. Naguleswaran A, Spicher M, Vonlaufen N, Ortega-Mora LM, Torgerson P, Gottstein B, et al. In vitro metacestodicidal activities of genistein and other isoflavones against *Echinococcus multilocularis* and *Echinococcus granulosus*. Antimicrob Agents Chemother. 2006;50 (11): 3770-8.
29. Orct T, Jurasovic J, Micek V, Karaica D, Sabolic I. Macro- and microelements in the rat liver, kidneys, and brain tissues; sex differences and effect of blood removal by perfusion in vivo. J Trace Elem Med Biol. 2017;40:104-11

30. Jung M, Jang HB, Lee SE, Park JH, Hwang YS. In vitro micro-mineralized tissue formation by the combinatory condition of adipose-derived stem cells, macroporous PLGA microspheres and a bioreactor. Macromolecular Research. 2013;22 1:47-57.
31. Mori F, Tanji K, Wakabayashi K. Widespread calcium deposits, as detected using the alizarin red S technique, in the nervous system of rats treated with dimethyl mercury. Neuropathology. 2000;20(3):210-5.
32. Xu B, Xing R, Huang Z, Yin S, Li X, Zhang L, et al. Excessive mechanical stress induces chondrocyte apoptosis through TRPV4 in an anterior cruciate ligament-transected rat osteoarthritis model. Life Sci. 2019;228:158-66.
33. Yang WR, Li BB, Hu Y, Zhang L, Wang XZ. Oxidative stress mediates heat-induced changes of tight junction proteins in porcine sertoli cells via inhibiting CaMKKβ-AMPK pathway. Theriogenology. 2020;142:104-13.
34. Maria AC, Celina EM. Efficacy of albendazole in combination with thymol against *Echinococcus multilocularis* protoscoleces and metacestodes. Acta Trop. 2014;140:61-7.
35. Diaz A, Casaravilla C, Irigoin F, Lin G, Previato JO, Ferreira F. Understanding the laminated layer of larval Echinococcus I: structure. Trends Parasitol. 2011;27 5:204-13.
36. Wang Y, Wang S, Pu Y, Zhu J, Zhao W. Observation of trace elements in serum of patients with hepatic echinococcosis. Journal of Ningxia Medical University. 2011;33(8):764-5. (in Chinese)
37. Vaeth M, Maus M, Klein-Hessling S, Freinkman E, Yang J, Eckstein M, et al. Store-Operated Ca(2+) Entry Controls Clonal Expansion of T Cells through Metabolic Reprogramming. Immunity. 2017;47 4:664-79.
38. Nawaratna SSK, You H, Jones MK, McManus DP, Gobert GN. Calcium and Ca(2+)/ Calmodulin-dependent kinase II as targets for helminth parasite control. Biochem Soc Trans. 2018;46(6):1743-51.

Tables

Table 1 Changes in the wet weight of *E. multilocularis* metacestodes in mice after treatment with verapamil for 4 months

Group	No. of mice	Dose	Cyst weight (g) (Mean ± SD)
Infected	5	NA	5.90 ± 0.75
ABZ	5	40 mg/kg/day	1.04 ± 0.14*
Vepm	5	40 mg/kg/day	0.98 ± 0.33*

Abbreviations: SD, standard deviation; NA, not available. Statistical analysis was performed by comparison with the infected group.

*$P < 0.05$.

Table 2 ICP-MS analysis of the calcium content in *E. multilocularis* infected mice after treatment with verapamil for 4 months

Sample	Calcium concentration (mg/L)		
	Uninfected group	Infected group [a]	Vepm group [b]
Serum	9.89 ± 1.92	4.92 ± 0.77*	6.39 ± 0.79
Liver	296.72 ± 9.43	172.72 ± 16.63*	226.78 ± 43.93*
Cysts	NA	3182.28 ± 190.77	3013.98 ± 115.80

Abbreviations: NA, not available.

[a] indicates the infected group vs. the uninfected group.

[b] indicates the vepm group vs. the infected group.

*$P < 0.05$.

Table 3 Analysis of CaM and CamK□ protein levels in *E. multilocularis* infected mice after oral administration of verapamil for 4 months by ELISA

Index	Sample	Uninfected group	Infected group [a]	Vepm group [b]
CaM (μg/mL)	Serum	13.81 ± 1.65	22.25 ± 5.55*	8.13 ± 1.26*
	Liver	3.42 ± 0.27	6.06 ± 1.83*	1.60 ± 0.68*
	Cysts	NA	2.36 ± 0.87	1.68 ± 0.10
CamK□ (ng/mL)	Serum	5.88 ± 0.99	22.87 ± 4.23*	5.13 ± 1.74*
	Liver	2.00 ± 0.61	4.25 ± 1.84*	1.97 ± 0.56*
	Cysts	NA	2.65 ± 1.24	1.79 ± 0.36

Abbreviations: NA, not available.

[a] indicates the infected group vs. the uninfected group.

[b] indicates the vepm group vs. the infected group.

*$P < 0.05$.

Figures

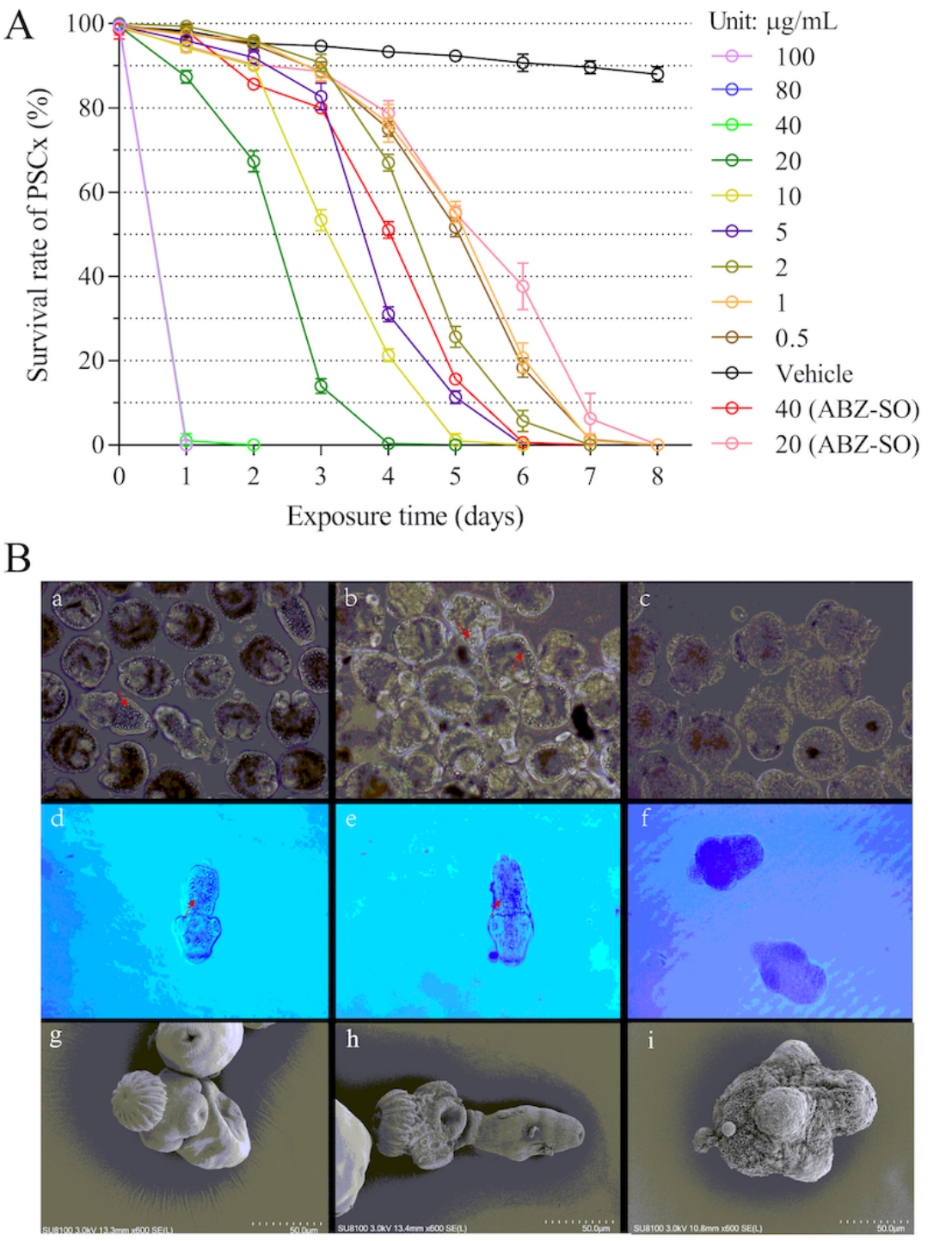

Figure 1

The effect of verapamil against E. granulosus protoscoleces in vitro. A. E. granulosus protoscoleces (PSC) were exposed to verapamil (vepm) at a concentration of 0.5-100 μg/mL, ABZ-SO at a concentration of 40 or 20μg/mL or 0.1% DMSO (the vehicle group) for 8 days. B. The morphological changes and ultrastructural alterations in PSC exposed to various drugs for 4 days were detected by light microscopy and SEM. a, d, g The typical morphology and structural integrity of PSC from the vehicle group; b, e, h

Mild morphological and structural alterations in the ABZ-SO (20 μg/mL) group. c, f, j Subatantial morphological and ultrastructural destruction in PSC exposed to vepm (20 μg/mL), including disappearance of calcareous corpuscles and hooks, shedding of the tegument and the presence of numerous blebs. a-c Light microscopy without any staining (200 × magnification); d-f Light microscopy with trypan blue staining (200 × magnification); g-i SEM (600 × magnification). The arrowhead (red) indicates an intact calcareous corpuscle.

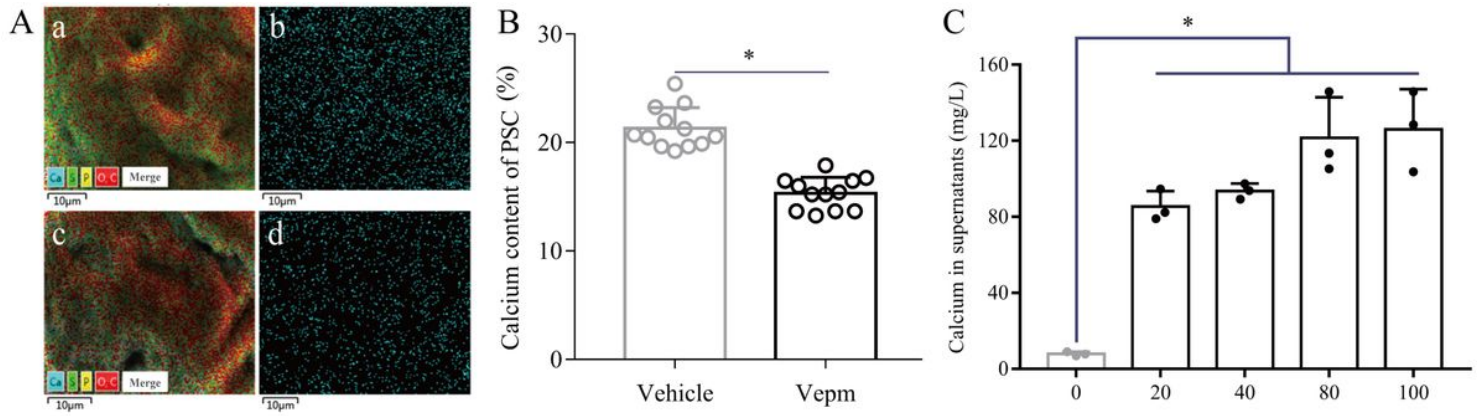

Figure 2

Changes in the calcium content in E. granulosus PSC after treatment with 20 μg/mL verapamil (vepm) for 4 days in vitro. A. Calcium distribution in E. granulosus PSC, as assayed by SEM-EDS. Merged image of multi-element (a, c) and calcium (b, d) distributions in PSC in the vehicle (a, b) and the vepm groups (c, d). B. The percentage of calcium content in E. granulosus PSC, as measured by SEM-EDS. C. The calcium content in the culture supernatants of E. granulosus PSC exposed to vepm (0, 20, 40, 80, 100 μg/mL), as measured by ICP-MS.

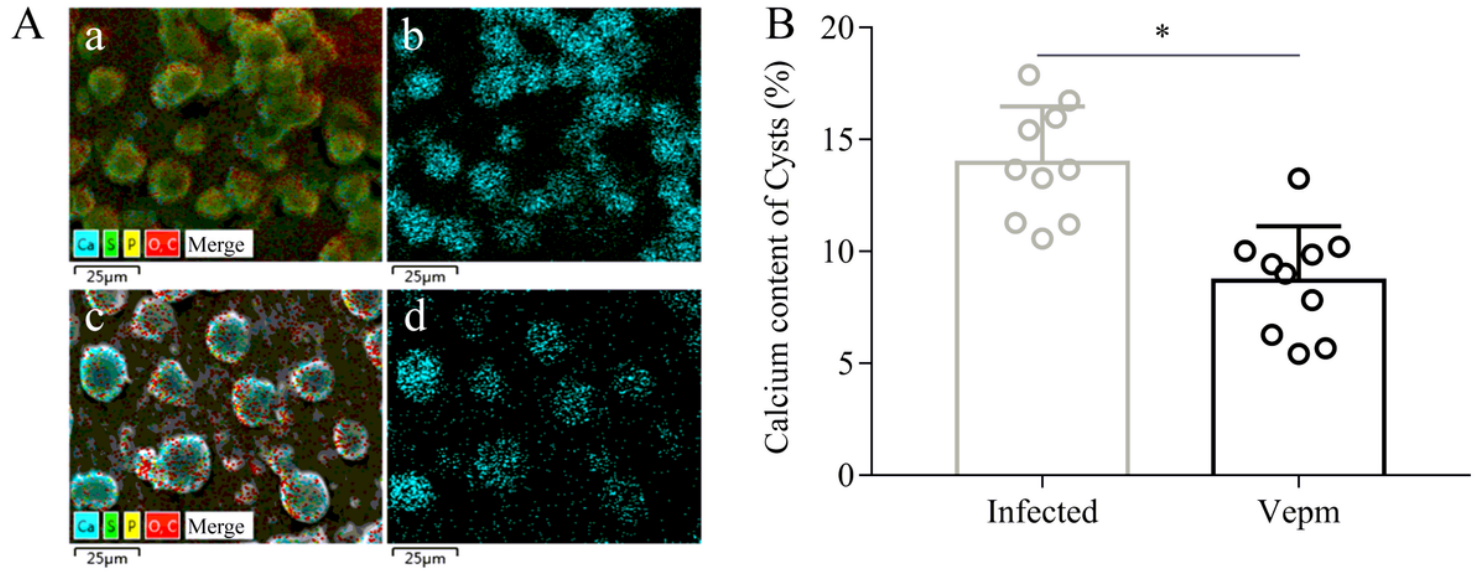

Figure 3

Changes in the calcium content of E. multilocularis-infected mice after treatment with 40 mg/kg verapamil (vepm) for 4 months, as measured by SEM-EDS. A. Calcium distribution in the germinal layer of E. multilocularis cysts. Merged image of multi-element (a, c) and calcium (b, d) distributions in the germinal layer of the infected (a, b) and vepm groups (c, d). B. The percentage of calcium content in the germinal layer of E. multilocularis metacestodes in mice after treatment with vepm.

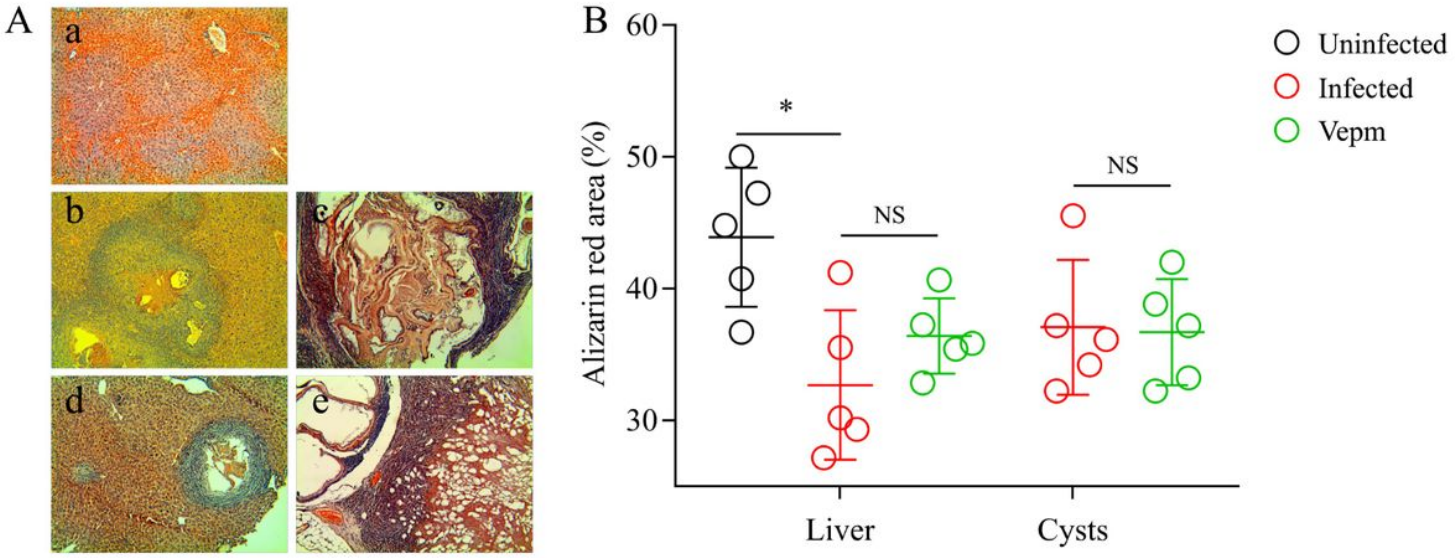

Figure 4

Changes in the calcium content in the liver and E. multilocularis cysts in mice after treatment with 40 mg/kg verapamil (vepm) for 4 months, as measured by Alizarin red staining. A. Calcium distribution in the liver (a, b, d) and E. multilocularis cysts (c, e) from uninfected (a), infected (b, c) and vepm-treated (d, e) mice (200 × magnification). B. Semiquantitative analysis of calcium content. NS, not significant.

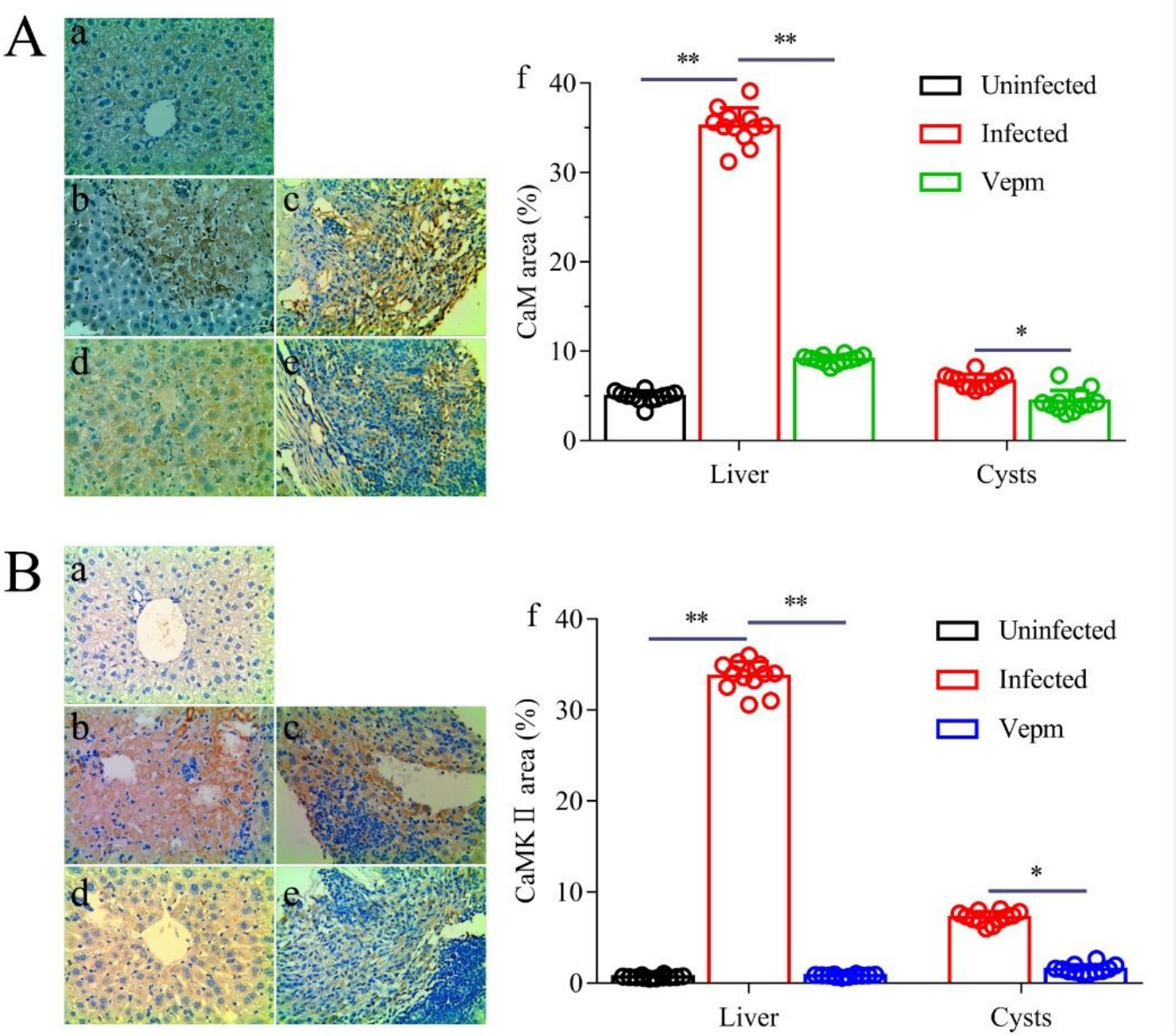

Figure 5

Analysis of CaM and Camk protein expression in the liver and E. multilocularis cysts after treatment with verapamil (vepm), as determined by paraffin immunohistochemistry. The protein expression of CaM (A) and CamK (B) in the livers (a, b, d) and E. multilocularis cysts (c, e) of uninfected (a), infected (b, c) and vepm-treated (d, e) mice (400 × magnification). f Semiquantitative analysis of CaM and CamK protein expression.

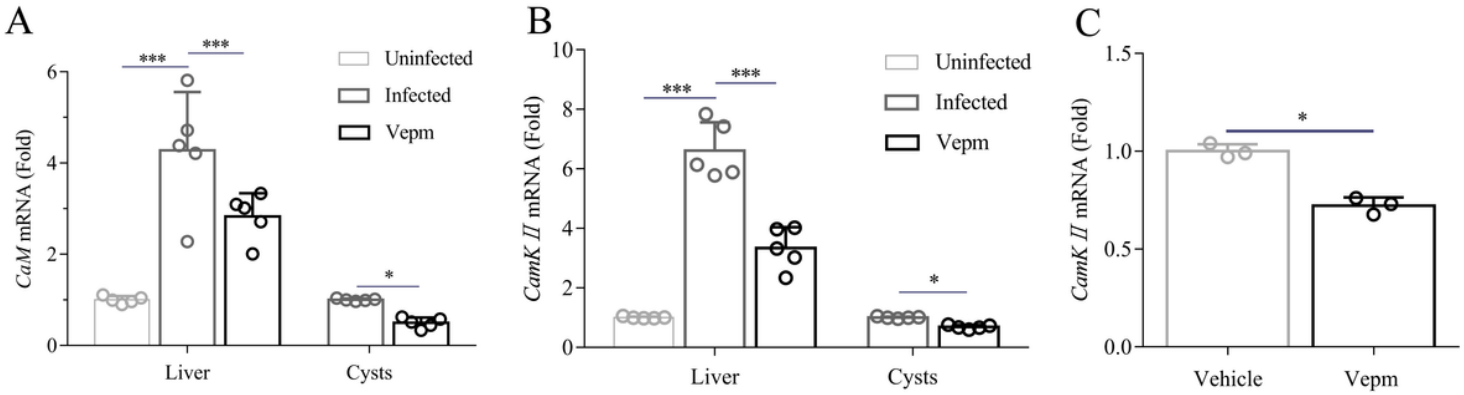

Figure 6

Expression of CaM and CamK mRNA in the livers and E. multilocularis cysts of mice after treatment with 40 mg/kg verapamil (vepm) for 4 months and in E. granulosus PSC after exposure to vepm (20 μg/mL) for 4 days, as measured by RT-qPCR. A. CaM mRNA expression. B. CamK mRNA expression. C. CamK mRNA expression in E. granulosus PSC.

Supplementary Files

This is a list of supplementary files associated with this preprint. Click to download.

- GraphicAbstract.tif